ORIGINAL PAPER



Crystal Structure and Preferential Site Occupancy in Cs₆Mn(H₂O)₂(VO₃)₈ and Cs₅KMn(H₂O)₂(VO₃)₈

Tiffany M. Smith Pellizzeri¹ · Colin D. McMillen¹ · Kimberly Ivey² · Joseph W. Kolis¹

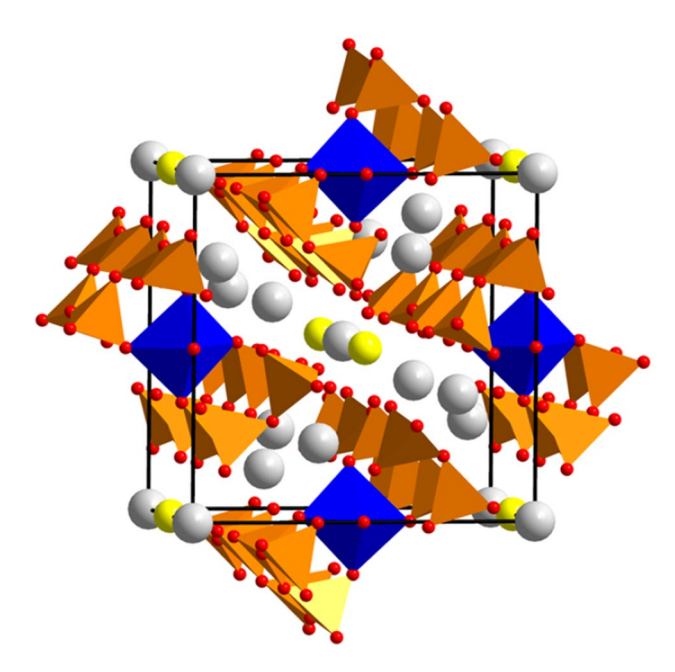
Received: 17 January 2019 / Accepted: 25 April 2019 / Published online: 18 May 2019 © Springer Science+Business Media, LLC, part of Springer Nature 2019

Abstract

Two new structurally related cesium manganese vanadates have been synthesized by a high-temperature (580 °C) hydrothermal synthetic method utilizing halide brine mineralizers. Both structures $Cs_6Mn(H_2O)_2(VO_3)_8$ (I) and $Cs_5KMn(H_2O)_2(VO_3)_8$ (II) are isostructural crystallizing in the tetragonal space group P4/mnc. The first structure, $Cs_6Mn(H_2O)_2(VO_3)_8$ (I) has unit cell dimensions of a=13.6830(4) Å, c=8.6476(3) Å and the second structure, $Cs_5KMn(H_2O)_2(VO_3)_8$ (II), has unit cell dimensions of a=13.5015(4) Å, c=8.5372(3) Å. The structures are built from a manganese vanadate chain, which consists of $[Mn(H_2O)_2O_4]$ units that are coordinated to one another by a unique sinusoidal vanadate chain, $(VO_3)_n$. Both structures have well-ordered alkali metal atoms, with the potassium atoms of II exhibiting preferential site occupancy. Both compounds were characterized by single crystal X-ray diffraction and infrared spectroscopy, to identify the characteristic O–H and V–O modes.

Graphical Abstract

Crystals of $Cs_6Mn(H_2O)_2(VO_3)_8$ and $Cs_5KMn(H_2O)_2(VO_3)_8$ were synthesized from hydrothermal brines and their structures determined by single crystal X-ray diffraction, revealing preferential, ordered site substitution of the alkali metals.



Keywords Hydrothermal synthesis · Metal vanadates · Brine mineralizers · Transition metal

Extended author information available on the last page of the article



Introduction

Transition metal vanadates are attractive systems to study because of their considerable structural complexity and potential applications [1-3]. Like silicate oxyanions, $(SiO_4)^{4-}$ [4, 5], vanadates readily form tetrahedral oxyanion building blocks $(VO_4)^{3-}$ [6–8]. Vanadates are of particular interest however, because of their structural flexibility, with the ability to adopt many different coordination geometries (i.e. four, five and six coordinate) while the vanadium ion can also assume a range of oxidation states ranging from 2 + to 5 + [9]. Vanadates can arrange themselves within structures to form chains, extended arrays, or even rings, leading to structural diversity in the crystalline products. Coordination of the vanadate oxyanion to open shell first row transition metals can also lead to magnetically interesting arrangements, such as magnetically coupled chains or spin frustrated triangles [6, 8, 10]. Our initial reactions in this phase space focused on manganese ions, due to their unusual magnetic properties and range of oxidation states and coordination environments [11, 12].

Traditionally, these types of materials are synthesized by high temperature (1000 °C) solid state methods [13–15]. However, our group has recently been concentrating on a high temperature hydrothermal route to access transition metal vanadate systems [9, 16–18]. Generally, these reactions are performed around 600 °C at pressures around 1.6 kbar. We found that hydrothermal synthesis usually leads to well-formed high-quality single crystals. We initially employed hydroxide mineralizers, but we have recently been turning our focus to systems that mimic natural brine environments. Therefore, we are exploring reactions in halide, or mixed halide/hydroxide mineralizers including BaCl₂ [9], BaF₂ [12], SrCl₂ [17], CsCl [19], and CsF [19] as well as combinations that also contain corresponding hydroxides. We see a wide range of behavior in the presence of halide salts in these reaction fluids. The halides perform multiple roles in that they serve as mineralizers but also play a role in the structural chemistry. In some cases we observe halide incorporation into the structure, while in others we see no halide incorporation in the lattice but do obtain products considerably different than those from pure hydroxide mineralizers. We find that the product distribution from our reactions is very dependent on the identity and concentration of the halide mineralizer, as well as whether any hydroxide is present with the halide. The alkali or alkaline earth metal component of the mineralizer system is similarly important in the crystal chemical behavior of the resultant products.

Herein we present two new manganese vanadates with related structures, synthesized from related reaction conditions. The first product, $Cs_6Mn(H_2O)_2(VO_3)_8$ (I) was

synthesized from cesium chloride, manganese (III) oxide, and vanadium (V) oxide in 1 M CsOH/3 M CsCl. The second product, $Cs_5KMn(H_2O)_2(VO_3)_8$ (II), was synthesized from cesium carbonate, manganese (IV) oxide, and vanadium (V) oxide in 3 M KCl. The backbone structure is the same in both cases, but one of the cesium cations is replaced with potassium in an ordered, site-specific manner in II. These two novel structures have been characterized through single-crystal X-ray diffraction, infrared spectroscopy, and EDX elemental analysis.

Experimental Section

Hydrothermal Crystal Growth of $Cs_6Mn(H_2O)_2(VO_3)_8$ (I) and $Cs_5KMn(H_2O)_2(VO_3)_8$ (II)

Hydrothermal reactions were conducted in 2.75-inch long silver tubes. Following the addition of the chloride or mixed chloride/hydroxide mineralizer (0.4 mL) to the silver tube, the reactants (~ 0.3 to 0.45 g total) were added. The silver tubes were then welded shut and placed in a Tuttle-seal autoclave. Distilled water was added to the autoclave to provide suitable counter pressure. The autoclaves were heated for 3-5 days and after cool down, the products were filtered via vacuum filtration and washed with water. The chemicals used in this study, cesium chloride (Alfa Aesar, 99.9%), cesium hydroxide solution, 50 wt% in water (Beantown Chemical, 99.9%), cesium carbonate (Alfa Aesar, 99.9%), potassium chloride (VWR, 99%), vanadium(V) oxide (Alfa Aesar, 99.6%), manganese(III) oxide (Strem Chemicals, 98%), and manganese(IV) oxide (Strem Chemicals, 99%) were used as received without further purification.

Single crystals of Cs₆Mn(H₂O)₂(VO₃)₈ (I) were prepared by using a mixture of cesium chloride (0.123 g, 0.731 mmol), manganese (III) oxide (0.0575 g, 0.364 mmol), and vanadium (V) oxide (0.265 g, 1.46 mmol) with 0.4 mL of 1 M CsOH/3 M CsCl mineralizer. The reaction was performed at 580 °C for 5 days at 1.7 kbar of pressure, and yielded yellow rod-shaped crystals of Cs₆Mn(H₂O)₂(VO₃)₈ (I), identified as a minor product of the reaction, along with colorless crystals of CsVO₃ [20] and black crystals identified as Mn_3O_4 [21]. Semiquantitative compositional data in atomic %, determined by EDX, was 52.2% O, 26.0% V, 18.5% Cs, and 3.3% Mn, indicating good agreement of the relative ratios of the heavy elements to the chemical formula determined from the structural analysis (expected, based on non-hydrogen atoms: 63.4% O, 19.5% V, 14.6% Cs, 2.4% Mn).

Single crystals of $Cs_5KMn(H_2O)_2(VO_3)_8$ (II) were produced from a reaction mixture of Cs_2CO_3 (0.134 g, 0.41 mmol), manganese(IV) oxide (0.029 g, 0.33 mmol), and vanadium(V) oxide (0.15 g, 0.825 mmol) with 0.4 mL



of 3 M KCl mineralizer at 500 °C for 3 days at 1.2 kbar of pressure. The new phase, $Cs_5KMn(H_2O)_2(VO_3)_8$ (II) was identified as yellow rod-shaped crystals as a minor product, along with black crystals identified as $K_2V_3O_8$ [22]. EDX confirmed the presence of potassium in II. Semiquantitative compositional data in atomic %, was 44.3% O, 30.1% V, 18.9% Cs and 3.8% K, and 2.9% Mn, also indicating good agreement of the relative ratios of the heavy elements to the chemical formula determined from the structural analysis (expected, based on non-hydrogen atoms: 63.4% O, 19.5% V, 12.2% Cs, 2.4% K, 2.4% Mn).

X-ray Diffraction

Well-formed single crystals of $Cs_6Mn(H_2O)_2(VO_3)_8$ (I) and $Cs_5K_1Mn(H_2O)_2(VO_3)_8$ (II) were used to perform single-crystal X-ray diffraction measurements. All data were collected at room temperature with a Bruker D8 Venture diffractometer having a Photon 100 detector, utilizing Mo K α radiation (λ =0.71073 Å) from an Incoatec I μ S source. Diffraction data were collected from φ and ω -scans. The APEXIII software suite was used for data collection, setup, and processing. The crystal structures were solved utilizing intrinsic phasing and full-matrix least square methods with refinement on F^2 . Structure refinements were

conducted using the SHELXTL software suite [23]. All of the atoms in each structure were first refined using isotropic thermal displacement parameters, followed by anisotropic refinement on all non-hydrogen atoms. Hydrogen atoms were identified from the difference electron density map and refined with distance fixing restraints in order to maintain an appropriate geometry for the coordinated water molecule. Since the parent oxygen atom of the water molecule is located on a four-fold symmetry site, the associated hydrogen atoms were set to partial occupancy at their general positions. Table 1 provides a summary of the structural refinement data for the compounds of this study and Table 2 lists selected interatomic bond distances and angles. Structural data have been deposited with the joint CCDC/FIZ Karlsruhe deposition service, deposition numbers 1890843 and 1890844.

Spectroscopic Characterization

Infrared Spectroscopy was performed on well-formed single crystals of (I) and (II). Single crystals of each compound were rolled out on a ZnSe plate, and the IR spectra were collected using 16 scans of the resultant sample. The IR samples were collected in the frequency range from 650

Table 1 Structure refinement data for $Cs_6Mn(H_2O)_2(VO_3)_8$ (I) and $Cs_5KMn(H_2O)_2(VO_3)_8$ (II)

	$\begin{array}{c} Cs_6Mn(H_2O)_2(VO_3)_8 \\ (I) \end{array}$	$\begin{array}{c} Cs_5KMn(H_2O)_2(VO_3)_8 \\ \textbf{(II)} \end{array}$	
Empirical Formula	$Cs_6MnV_8O_{26}H_4$	Cs ₅ KMnV ₈ O ₂₆ H ₄	
F. W. (g/mol)	1679.95	1586.14	
Temperature (K)	298 (2)	298 (2)	
Crystal System	Tetragonal	Tetragonal	
Space group	P4/mnc	P4/mnc	
a (Å)	13.6830 (4)	13.5015 (4)	
c (Å)	8.6476 (3)	8.5372 (3)	
Volume (Å ³)	1619.04 (11)	1556.25 (11)	
Z	2	2	
D(calcd)(g/cm ³)	3.446	3.385	
$\mu (mm^{-1})$	9.308	8.664	
F(000)	1502	1430	
Crystal size (mm)	$0.06 \times 0.08 \times 0.20$	$0.04 \times 0.06 \times 0.23$	
2θ range (°)	2.79 to 26.50	2.832 to 26.486	
Reflections collected	11,654	10,907	
Indep. Reflections	905	864	
R indices $(I > 2\sigma(I))$	$R_1^{\rm a} = 0.0373, wR_2^{\rm b} = 0.0857$	$R_1^a = 0.0237, wR_2^b = 0.0510$	
R indices (all data)	$R_1^a = 0.0435, wR_2^b = 0.0878$	$R_1^{\rm a} = 0.0297, wR_2^{\rm b} = 0.0528$	
Goodness of fit (S)	1.226	1.163	

$${}^{a}R_{1} = \sum \|F_{o}| - [F_{c} \| / \sum |F_{o}| \\ {}^{b}wR_{2} = \left\{ \sum w(F_{o}^{2} - F_{c}^{2})^{2} / \sum [w(wF_{o}^{2})^{2}] \right\}^{1/2}$$



Table 2 Selected interatomic distances (Å) and angles (°) for $Cs_6Mn(H_2O)_2(VO_3)_8$ (I) and $Cs_5KMn(H_2O)_2(VO_3)_8$ (II)

$Cs_6Mn(H_2O)_2(VO_3)_8$ (I)		$Cs_5KMn(H_2O)_2(VO_3)_8$ (II)	
Cs1-O2 × 8	2.920(5)	K1-O2 ×8	2.792(3)
$Cs2-O4 \times 2$	3.205(5)	$Cs2-O4 \times 2$	3.137(3)
$Cs2-O3 \times 2$	3.351(6)	$Cs2-O3 \times 2$	3.257(3)
$Cs2-O2 \times 4$	3.496(7)	$Cs2-O2 \times 4$	3.392(3)
$Cs2-O4 \times 2$	3.525(6)	$Cs2-O4 \times 2$	3.503(3)
Cs2-O5w	3.6021(8)	Cs2–O5w	3.5686(4)
Cs3–O1 \times 4	3.115(8)	Cs3–O1 \times 4	3.004(4)
$Cs3-O2 \times 8$	3.579(7)	$Cs3-O2 \times 8$	3.519(3)
V1-O1	1.795(3)	V1-O1	1.8016(16)
V1-O2	1.617(6)	V1-O2	1.622(3)
V1-O3	1.795(3)	V1-O3	1.8009(16)
V1-O4	1.643(5)	V1-O4	1.650(3)
$Mn1-O4 \times 4$	2.205(5)	$Mn1-O4 \times 4$	2.216(3)
$Mn1-O5w \times 2$	2.16,190(8)	$Mn1-O5w \times 2$	2.13430(8)
V1-O3-V1	135.7(5)	V1-O3-V1	136.1(2)
V1-O4-Mn1	132.4(3)	V1-O4-Mn1	132.47(17)

to 4000 cm⁻¹ at a resolution of 4 cm⁻¹ using a Thermo-Nicolet Magna 550 FTIR equipped with a Thermo-Nicolet NicPlan FTIR microscope and a MCT/A detector.

Results and Discussion

Crystal Structures of $Cs_6Mn(H_2O)_2(VO_3)_8$ (I) and $Cs_5KMn(H_2O)_2(VO_3)_8$ (II)

The two compounds discussed herein, (I) and (II), are isomorphous, having the same general structural features except the site-specific potassium occupancy discussed below for II. Both structures are built from sinusoidal vanadate chains coordinated to one another through

octahedral manganese atoms, forming a one-dimensional manganese vanadate chain. The cesium (or cesium and potassium ions in the case of **II**) ions provide charge-balance to the manganese vanadate chains and reside in the void spaces in the structures between the chains (Fig. 1).

There is one unique manganese atom in structure, Mn1, occupying a 4d Wyckoff site (222 symmetry). During the initial refinements, the anisotropic displacement parameters for Mn1 were found to be unusually high. The Mn1 atom was then set to half occupancy, greatly improving the refinement statistics, and ultimately providing appropriate charge balance as Mn²⁺. The partial occupancy of this site is also important sterically, as the alternating absence of half of the Mn atoms along the manganese vanadate chains provides the necessary space for the hydrogen atoms of the coordinated water molecules (Fig. 2). The manganese site is six-coordinate with oxygen, as [MnO₄(H₂O)₂] units, having the water molecules at axial positions and corner-shared oxygen atoms with the vanadate chains at equatorial positions. This arrangement results in manganese atoms that are isolated from one another and only linked over long range via bridging of the vanadate chain (Fig. 2). The Mn–O bond lengths are consistent with Mn²⁺, as is the yellow color of the crystals.

There is one unique vanadium atom in the structure, V1, which is four-coordinate with oxygen. It is coordinated by two oxygen atoms propagating the metavanadate chain (O3 and O1), one oxygen atom coordinated to the manganese octahedron (O4), and one terminal oxygen atom (O2). When the Mn atom is absent in the chain due to its partial occupancy, the O4 atom also becomes a terminal oxygen atom. In these instances it acts as a hydrogen bond acceptor for the hydrogen atoms of the water molecule (H···A = 1.90(2) Å; D···A = 2.823(5) Å; D-H···A = 176(4)°). The longest V-O bonds are the bridging V-O-V bonds, which average 1.8013(16) Å. The shortest V-O bond is the always-terminal bond at 1.622(3) Å. The metavanadate chain takes on a

Fig. 1 View along the c-axis in $Cs_6Mn(H_2O)_2(VO_3)_8$ (I) (left) and $Cs_5KMn(H_2O)_2(VO_3)_8$ (II) (right). Hydrogen atoms are removed for clarity. Color scheme: Cesium (grey), potassium (yellow), manganese (blue octahedra), vanadium (orange tetrahedra), and oxygen (red spheres) (Color figure online)

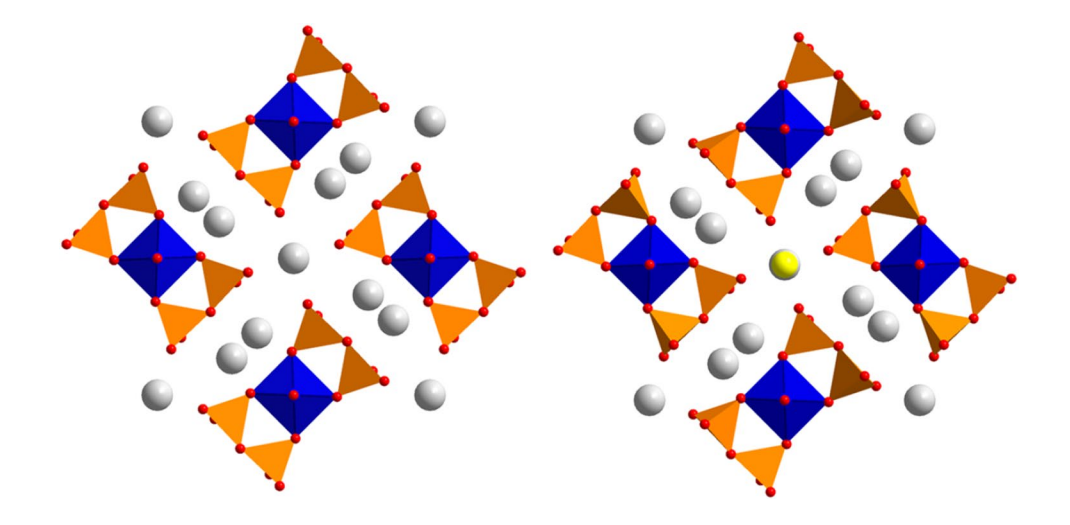
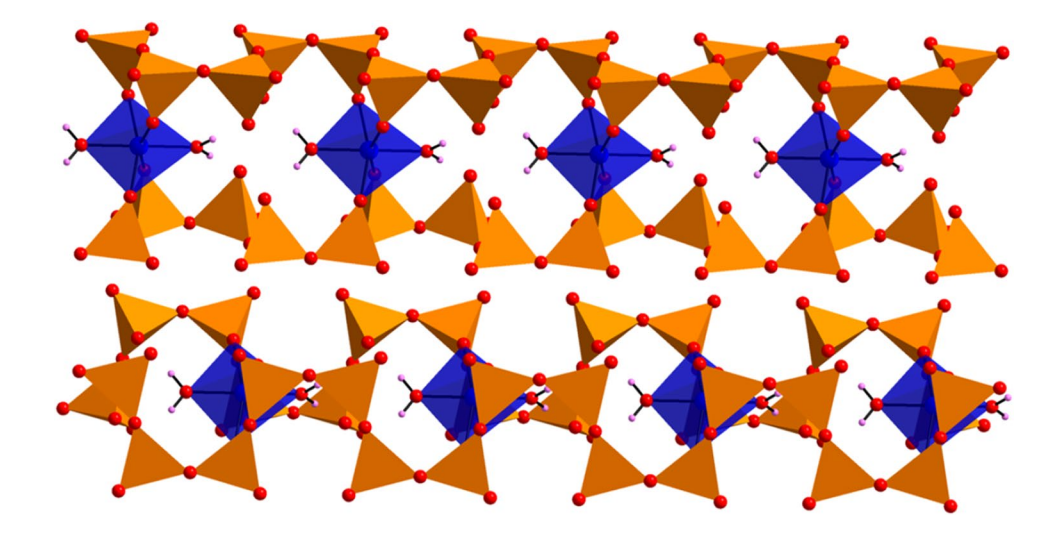




Fig. 2 The backbone manganese vanadate chain present in both (I) and (II). See Fig. 1 for color scheme. Hydrogen atoms are shown as pink spheres (Color figure online)



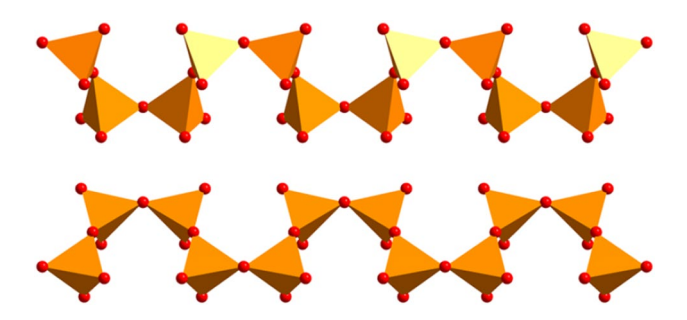
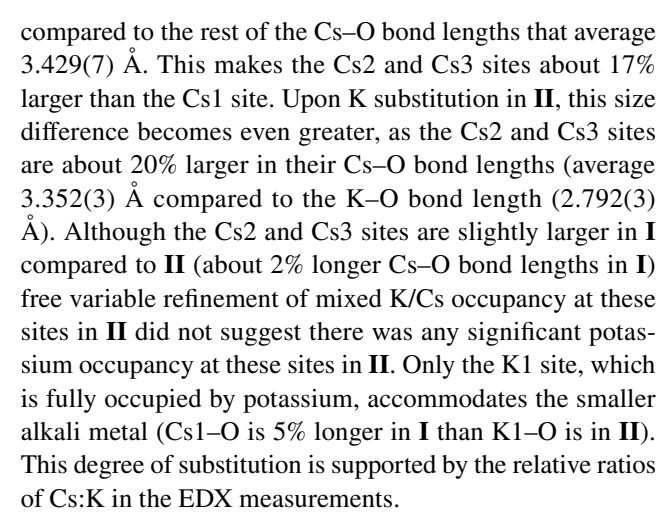


Fig. 3 The sinusoidal vanadate $(VO_3)_n$ chains in (I) and (II) along the *a*-axis. Color scheme is the same as Fig. 1 (Color figure online)

rather unique sinusoidal shape. This type of chain is generally quite rare in solid-state structures, but we have seen it in some of our previous work, namely $Cs_3Mn(VO_3)_4Cl$ [19]. The V–O–V angle in $Cs_3Mn(VO_3)_4Cl$ is $142.1(4)^\circ$, and the V–O–V angle in **I** and **II** averages $135.9(4)^\circ$. Zig–zagging metavanadate chains typically have V–O–V angles in the range of $160-170^\circ$ [24], however as we see here, the sinusoidal shape results in a much more relaxed V–O–V angle (Fig. 3).

Alkali Metal Site Specificity

The Cs atoms of **I** occupy three unique Wyckoff sites: Cs1 at a 2b site, Cs2 at a 8h site, and Cs3 at a 2a site. Interesting site-specific substitution was observed when KCl was used as a mineralizer to synthesize the mixed alkali metal isomorph $Cs_5KMn(H_2O)_2(VO_3)_8$ (**II**). In **II**, a potassium atom replaces only the Cs atom at the 2b site, accounting for the one potassium atom per formula unit. Based on the bond lengths observed in Table 2, it is clear that the Cs1/2b site would preferentially accommodate substitution of the smaller K atom given its much shorter bond lengths to oxygen. The Cs–O bond length of Cs1 in **I** is 2.920(5) Å,



The K1 site is located at the center of four manganese vanadate chains (Fig. 4), coordinating eight of the terminal O₂ atoms from these chains. Effectively, this smaller cation draws all the chains closer together in **II** compared to **I**, thus accounting for some measurable contraction of the Cs–O bond lengths even on sites that are not substituted by K. The K1 and Cs3 sites occur in alternating fashion along the *c*-axis in the channels between four metavanadate chains (Figs. 1, 4), while the Cs2 sites are sandwiched between three metavanadates from two manganese vanadate chains.

Infrared Spectroscopy

The infrared spectra of **I** and **II** are shown in Fig. 5. Both compounds display the characteristic broad O–H symmetric and asymmetric stretching band at $\sim 3186 \text{ cm}^{-1}$ for **I** and at $\sim 3211 \text{ cm}^{-1}$ for compound **II**. Furthermore, the O–H bending modes of the coordinated H₂O group can be identified at $\sim 1660 \text{ cm}^{-1}$ for **I** and $\sim 1652 \text{ cm}^{-1}$ for **II**. The characteristic V–O stretches can also be identified from the region between 1000 and 700 cm⁻¹. The IR bands $\sim 956 \text{ cm}^{-1}$ and



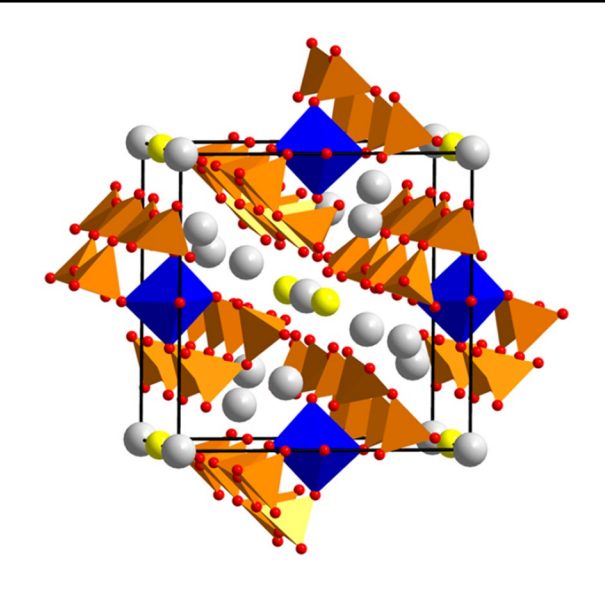
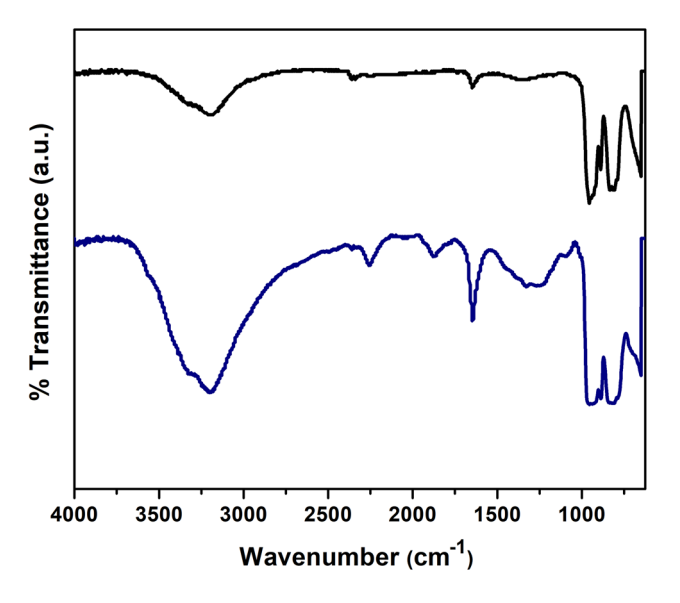


Fig. 4 Extended unit cell of **II** viewed slightly off the c-axis, showing site-specific potassium substitution (yellow spheres). Color scheme is the same as Fig. 1 (Color figure online)



 $\textbf{Fig. 5} \quad \text{Infrared spectra of } I \text{ (black) and } II \text{ (blue) (Color figure online)}$

 $827~\rm cm^{-1}$ can both be assigned to the VO_2 stretching mode, while, the IR peak at ~ $640~\rm cm^{-1}$ is assigned to the V–O–V stretching vibration [25]. The similarities in the characteristic vibrational frequencies for I and II suggest that the metavanadate chains themselves are not especially influenced by the site specific alkali metal substitution. This is also supported by the crystallographic comparison of the bond lengths and angles.

Conclusions

Herein we have reported the structures of two new manganese vanadates, namely Cs₆Mn(H₂O)₂(VO₃)₈ (I) and Cs₅KMn(H₂O)₂(VO₃)₈ (II), synthesized from hydrothermal brines. Both compounds were analyzed by single crystal X-ray diffraction, infrared spectroscopy, and elemental analysis by EDX. The structural backbone in both structures is built from manganese vanadate chains. The manganese atoms themselves do not form an extended chain, but are flanked by sinusoidal vanadate chains, $(VO_3)_n$, to create the one-dimensional chains with isolated manganese octahedra linked by the vanadate chains. The isolated manganese octahedra resulting from their half occupancy are necessary to account for the coordinated water molecules on the [MnO₄(H₂O)₂] octahedra, the presence of which was verified by the infrared spectra. The use of KCl as the mineralizer led to the formation of II, where potassium atoms preferentially occupy one crystallographic site. The preferred site for potassium occupancy sits in channels between four manganese vanadate chains. This site has a significantly contracted coordination sphere to oxygen compared to the other cesium sites in the structure, which do not accommodate any potassium ions. The variety of synthetic and structural chemistry observed to occur from these hydrothermal brines is promising for continued study.

Acknowledgements We are indebted to the National Science Foundation NSF-DMR-1808371 for financial support of this work.

References

- Livage J (1998) Synthesis of polyoxovanadates via "chimie douce". Coord Chem Rev 178–180:999–1018. https://doi. org/10.1016/S0010-8545(98)00105-2
- Chirayil T, Zavalij PY, Whittingham MS (1998) Hydrothermal synthesis of vanadium oxides. Chem Mater 10:2629–2640. https://doi.org/10.1021/cm980242m
- Schindler M, Hawthorne FC, Baur WH (2000) A crystal-chemical approach to the composition and occurrence of vanadium minerals. Can Miner 38:1443–1456. https://doi.org/10.2113/gscan min.38.6.1443
- McMillen CD, Kolis JW (2016) Hydrothermal synthesis as a route to mineralogically-inspired structures. Dalton Trans 45:2772– 2784. https://doi.org/10.1039/C5DT03424H
- Liebau F (1985) Structural chemistry of silicates—structure, bonding, and classification. Springer Science & Business Media, New York
- Möller A, Amuneke NE, Daniel P, Lorenz B, de la Cruz CR, Gooch M, Chu PCW (2012) A Ag₂M[VO₄]₂ (A=Ba, Sr; M=Co, Ni): a series of ferromagnetic insulators. Phys Rev B 85:214422. https://doi.org/10.1103/PhysRevB.85.214422
- Lawes G, Harris AB, Kimura T, Rogado N, Cava RJ, Aharony A, Etin-Wohlman O, Yildirim T, Kenzelmann M, Broholm C, Ramirez AP (2005) Magnetically driven ferroelectric order in



- $\rm Ni_3V_2O_8.$ Phys Rev Lett 95:087205. https://doi.org/10.1103/PhysRevLett.95.087205
- 8. Bellido N, Martin C, Simon C, Maignan A (2007) Coupled negative magnetocapacitance and magnetic susceptibility in a Kagomé staircase-like compound ${\rm Co_3V_2O_8}$. J Phys 19:056001. https://doi.org/10.1088/0953-8984/19/5/056001
- Smith Pellizzeri TM, McMillen CD, Wen Y, Chumanov G, Kolis JW (2017) Three unique barium manganese vanadates from high-temperature hydrothermal brines. Inorg Chem 56:4206–4216. https://doi.org/10.1021/acs.inorgchem.7b00229
- Clemens O, Rohrer J, Nénert G (2016) Magnetic structures of the low temperature phase of Mn₃(VO₄)₂—towards understanding magnetic ordering between adjacent Kagomé layers. Dalton Trans 45:156–171. https://doi.org/10.1039/C5DT03141A
- Sanjeewa LD, McGuire MA, McMillen CD, Willett D, Chumanov G, Kolis JW (2016) Honeycomb-like S = 5/2 spin-lattices in manganese(II) vanadates. Inorg Chem 55:9240–9249. https://doi.org/10.1021/acs.inorgchem.6b01286
- Sanjeewa LD, McMillen CD, McGuire MA, Kolis JW (2016) Manganese vanadate chemistry in hydrothermal BaF₂ brines: Ba₃Mn₂(V₂O₇)₂F₂ and Ba₇Mn₈O₂(VO₄)₂F₂₃. Inorg Chem 55:12512–12515. https://doi.org/10.1021/acs.inorgchem.6b02355
- Erdei S (1993) Growth of oxygen deficiency-free YVO₄ single crystal by top-seeded solution growth technique. J Cryst Growth 134:1–13. https://doi.org/10.1016/0022-0248(93)90002-E
- Erdei S, Johnson GG, Ainger FW (1994) Growth studies of YVO₄ crystals (II). Changes in Y–V–O-stoichiometry. Cryst Res Technol 29:815–828. https://doi.org/10.1002/crat.2170290610
- 15. Wang N, He Z, Cui M, Guo W, Zhang S, Yang M (2015) Syntheses and Characterization of a Family of Vanadate Compounds $Ba_3M(V_2O_7)_2\ (M=Co,\ Mn,\ Mg,\ or\ Zn)\ with\ an\ Edge-Shared \\ [M_2O_{10}]\ Dimer\ Structure.\ Cryst\ Growth\ Des\ 15:1619–1624.\ https://doi.org/10.1021/cg5012814$
- Sanjeewa LD, McGuire MA, Smith Pellizzeri TM, McMillen CD, Garlea VO, Willett D, Chumanov G, Kolis JW (2016) Synthesis and characterization of new fluoride-containing manganese vanadates A₂Mn₂V₂O₇F₂ (A = Rb, Cs) and Mn₂VO₄F. J Solid State Chem 241:30–37. https://doi.org/10.1016/j.jssc.2016.05.008
- Smith Pellizzeri TM, McMillen CD, Pellizzeri S, Wen Y, Getman RB, Chumanov G, Kolis JW (2017) Strontium manganese vanadates from hydrothermal brines: synthesis and structure of

- $Sr_2Mn_2(V_3O_{10})(VO_4)$, $Sr_3Mn(V_2O_7)_2$, and $Sr_2Mn(VO_4)_2(OH)$. J Solid State Chem 255:225–233. https://doi.org/10.1016/j.issc.2017.07.008
- 18. Sanjeewa LD, McGuire MA, Garlea VO, Hu L, Chumanov G, McMillen CD, Kolis JW (2015) Hydrothermal synthesis and characterization of novel brackebuschite-type transition metal vanadates: Ba₂M(VO₄)₂(OH), M=V³⁺, Mn³⁺, and Fe³⁺, with interesting Jahn-Teller and spin-liquid behavior. Inorg Chem 54:7014–7020. https://doi.org/10.1021/acs.inorgchem.5b01037
- Pellizzeri TMS, McGuire MA, McMillen CD, Wen Y, Chumanov G, Kolis JW (2018) Two halide-containing cesium manganese vanadates: synthesis, characterization, and magnetic properties. Dalton Trans 47:2619–2627. https://doi.org/10.1039/C7DT0 4642A
- Hawthorne FC, Calvo C (1977) The crystal chemistry of the M⁺VO₃ (M⁺=Li, Na, K, NH₄, Tl, Rb, and Cs) pyroxenes. J Solid State Chem 22:157–170. https://doi.org/10.1016/0022-4596(77)90033-0
- Boucher B, Buhl R, Perrin M (1971) Proprietes et structure magnetique de Mn₃O₄. J Phys Chem Solids 32:2429–2437. https://doi.org/10.1016/S0022-3697(71)80239-1
- Galy J, Carpy A (1975) Structure cristalline de K₂V₃O₈ ou K₂(VO)[V₂O₇]. Acta Crystallogr B 31:1794–1795. https://doi.org/10.1107/S0567740875006231
- Sheldrick GM (2015) Crystal structure refinement with SHELXL. Acta Crystallogr Sect C Struct Chem 71:3–8. https://doi. org/10.1107/S2053229614024218
- Queen WL, West JP, Hwu S-J, VanDerveer DG, Zarzyczny MC, Pavlick RA (2008) The versatile chemistry and noncentrosymmetric crystal structures of salt-inclusion vanadate hybrids. Angew Chem Int Ed 47:3791–3794. https://doi.org/10.1002/anie.20070 5113
- Onodera S, Ikegami Y (1980) Infrared and Raman spectra of ammonium, potassium, rubidium, and cesium metavanadates. Inorg Chem 19:615–618. https://doi.org/10.1021/ic50205a008

Publisher's Note Springer Nature remains neutral with regard to jurisdictional claims in published maps and institutional affiliations.

Affiliations

Tiffany M. Smith Pellizzeri¹ · Colin D. McMillen¹ · Kimberly Ivey² · Joseph W. Kolis¹

- Department of Chemistry and Center for Optical Materials Science and Engineering Technologies (COMSET), Clemson University, 485 H.L. Hunter Laboratories, Clemson, SC 29634-0973, USA
- Department of Materials Science and Engineering, Clemson University, Clemson, SC 29634-0973, USA

